



# Total alkylated polycyclic aromatic hydrocarbon characterization and quantitative comparison of selected ion monitoring versus full scan gas chromatography/mass spectrometry based on spectral deconvolution

Christian Zeigler<sup>a</sup>, Kevin MacNamara<sup>b</sup>, Zhendi Wang<sup>c</sup>, Albert Robbat Jr.<sup>a,\*</sup>

<sup>a</sup> Tufts University, Chemistry Department, 62 Talbot Avenue, Medford, MA 02144, USA

<sup>b</sup> Irish Distillers-Pernod Ricard, Midleton Distillery, Midleton, Cork, Ireland

<sup>c</sup> Emergencies Science and Technology Division, Environment Canada, Environmental Technology Center, 3439 River Road, Ottawa, Ontario K1A 0H3, Canada

## ARTICLE INFO

### Article history:

Received 2 May 2008

Received in revised form 7 July 2008

Accepted 15 July 2008

Available online 3 August 2008

### Keywords:

Automated sequential 2D GC–GC/MS

Alkylated PAH

Ion Signature deconvolution software

Environmental forensics

Diesel

Petroleum

## ABSTRACT

Quantitative information of alkylated PAH is frequently used in forensic investigations to characterize petroleum releases and fate in the environment. Interference from a complex matrix often obviates target compound quantitation. Using single ion SIM or a single mass spectral pattern to analyze these homologs should result in either over- or underestimating their concentration. To confirm this hypothesis, a library of C<sub>1</sub>–C<sub>4</sub> alkylated PAH fragmentation patterns were made from automated sequential two-dimensional GC–GC/MS data and the Ion Signature deconvolution software. Based on these patterns, 1D GC/MS data was compared using single ion extraction and one fragmentation pattern per homolog against data obtained from those peaks whose scans met the spectral deconvolution criteria. Significant overestimation occurs when a single ion is used to extract peak signal for C<sub>4</sub>-naphthalene, C<sub>1</sub>-fluorene, and the C<sub>1</sub>- to C<sub>3</sub>-dibenzothiophenes. In contrast, C<sub>2</sub>-naphthalene, C<sub>2</sub>-fluorene, C<sub>3</sub>-phenanthrene, and C<sub>1</sub>-dibenzothiophene were underestimated by >50% when one fragmentation pattern per homolog was used. The Ion Signature deconvolution software makes it easy to interpret mass spectrometry data, especially in complex environmental samples like diesel fuel.

© 2008 Elsevier B.V. All rights reserved.

## 1. Introduction

Forensic environmental investigations rely on information gleaned from quantitative measurements of specific chemicals or families of chemically related compounds. This information is used to distinguish contaminant source (e.g. petroleum, coal tar, fire debris) as well as degradation, evaporation, or washing rates due to interactions with the environment [1,2]. For fossil fuels these include benzene [2,3], benzothiophenes [4], polycyclic aromatic hydrocarbons (PAHs) [5], and their alkylated analogs (C<sub>1</sub>–C<sub>4</sub>, saturated side chains) as well as *n*-alkanes, diamondoids [6], hopanes [7], steranes [8], terpanes and their derivatives [9]. These compounds are used to identify and differentiate the source, determine risk to human health and the environment, and to direct remedial efforts and assign blame [10].

The most often used separation technique in these investigations is gas chromatography (GC). When GC is combined with a flame ionization detector (FID), the ability to identify key con-

stituents is compromised due to the complexity of the sample and the universal response of the detector. Recently, an attractive alternative to increase the depth of information provided by GC-FID has been developed. In comprehensive GC, GC × GC, the two columns are linked by a modulator so that first column effluent is refocused and transferred in sharp concentration pulses to the second column [11–16]. Although this technique requires additional equipment and specialized software to visualize the data, separation efficiencies are dramatically increased when two orthogonally phased GC columns are used. With FID, GC × GC only allows the analyst to identify classes of compounds based upon their retention in the two phases, e.g., single and multiple ring aromatics and saturates.

Selective sulfur chemiluminescence detectors have also been used [17,18]. While sulfur-specific detectors can eliminate matrix interferences inherent in FID and mass spectrometry (MS), they cannot provide unambiguous identification without confirmation. Because benzothiophenes are among the only sulfur-containing compounds of interest, sulfur-selective detectors have found limited use in forensic analyses.

GC/MS is the most often used technique. It can provide positive identification but only when the mass spectrum for a given

\* Corresponding author. Tel.: +1 617 627 3474; fax: +1 617 627 3443.

E-mail address: [albert.robbat@tufts.edu](mailto:albert.robbat@tufts.edu) (A. Robbat Jr.).

sample component is unencumbered by coeluting compounds. Spectra of known compounds are stored in NIST, Wiley or user-specific libraries and then compared against spectra from the sample to identify target compounds or unknowns. Although GC/MS is an extremely powerful tool, unresolved fossil fuel chromatograms make the standard statistical sample and library matching algorithms ineffective.

To circumvent this problem, it is common practice to employ selective ion monitoring (SIM) mass spectrometry [2,19–23]. In this mode, the MS is typically set to acquire one or two ions per compound. SIM has become the preferred detection method because it provides increased measurement sensitivity over full scan MS. In single ion SIM, compound identification is predicated solely on retention times. Little advantage is gained over FID, with common ion effects from the matrix resulting in overestimation of the target compound. Use of a single confirming ion offers little additional informational value, especially where  $m/z$  isomer ion ratios differ by more than 20% and when the matrix contributes to a common ion. For example, base and confirming ions for 1-ethylnaphthalene and 2,3-dimethylnaphthalene are 141 (100%) and 156 (50%) and 141 (100%) and 156 (100%), respectively. Analysts will either accept both compounds as present because base and confirming ions co-maximize or ignore the second isomer as a matrix interferent because its relative abundance differs from the first by more than 20%. If both compounds are deemed present, the same response factor is used, which may not be appropriate. If only one compound is considered present, total C<sub>2</sub>-naphthalenes will be underestimated.

Recently, we published the results of a high temperature transfer line coupled to a membrane inlet probe on one end and either a photoionization detector or freeze-trap on the other for detecting PAH in the subsurface [24]. The aim was to quantitatively identify PAH without bringing soil or aqueous samples to the surface and to demonstrate that conventionally collected samples whether analyzed in the field or laboratory produced statistically equivalent data when compared to EPA method 8270. Results showed field and lab data were comparable and well within EPA benchmarks for precision and accuracy except for the alkylated PAH analogs. Except for alkylated PAH, we showed excellent results could be produced in the field quickly enough to support on-site decision making. On the other hand, the poorer alkylated PAH data led us to investigate why these compounds were not quantitated correctly.

In this paper, we address why discrepancies occur in alkylated PAH results independent of whether samples are analyzed by SIM or full scan mass spectrometry. NIST and Wiley mass spectral libraries and automated sequential GC–GC/MS with spectral deconvolution were used to build libraries of alkylated PAH fragmentation patterns for each C<sub>1</sub>–C<sub>4</sub> naphthalene, fluorene, phenanthrene, and dibenzothiophene analog. GC–GC is also a “comprehensive” technique in that automated sequential heart-cuts allow all of the first column effluent to be subjected to second column separation mechanisms and that complete separation of individual compounds and/or classes of compounds is often possible. GC–GC is the preferred multidimensional technique when building libraries from complex samples. Because of the much longer, independently heated second column, this technique offers the best opportunity to separate aromatics from saturates and, at the same time, provides wide enough peak bandwidths so that quadrupole mass filters can be used. In an earlier publication, we demonstrated the utility of this approach for obtaining pure mass spectra and building MS libraries from essential oils used to make gin [25]. Once the library of patterns is found for each C<sub>1</sub>–C<sub>4</sub> alkylated PAH, mass spectral deconvolution of one-dimensional GC/MS data is performed. Spectral deconvolution allows the analyst to “pull out” the correct mass spectrum for the targeted compound from extremely

complex matrixes [26–28]. Finally, we compare the mass spectral deconvolution results against SIM.

## 2. Experimental

### 2.1. Standards and reagents

A diesel fuel #2 standard was obtained from Restek (Bellefonte, PA) and used as received. Naphthalene, 1-ethylnaphthalene, 1,2-dimethylnaphthalene, and 2,3-dimethylnaphthalene were purchased from Sigma–Aldrich (St. Louis, MO), diluted with HPLC, GC/MS grade methylene chloride (Fischer, Fair Lawn, NJ) to prepare 5, 10, 50, 100, and 250 ppm standards, which were used to calculate response factors. Internal standards, naphthalene-d<sub>8</sub> and acenaphthene-d<sub>10</sub>, were also purchased from Restek Corporation, used as received, made to contain 50 ppm in each calibration standard. Response factors were calculated as the ratio of  $A_x C_{is} / A_{is} C_x$ , where  $C_x$  was the amount of target analyte injected and  $A_x$  the observed signal.  $C_{is}$  and  $A_{is}$  were the corresponding internal standard concentration and signal response.

### 2.2. Gas chromatography/mass spectrometry

For all 1D and GC–GC/MS analyses, the MS was scanned from 35 to 550  $m/z$ , with a 150-threshold count and 1.00 min solvent delay. The quadrupole was held at 150 °C, with the ion source at 230 °C. The Ion Fingerprint Detection algorithms, developed at Tufts University (Medford, MA), were incorporated into fully functional data analysis software by Ion Signature Technology (North Smithfield, RI) and used throughout this investigation. The NIST (Gaithersburg, MD) Mass Spectral Search Program v 2.0 was used to identify possible alkylated PAH in the GC–GC/MS cuts.

The Agilent model 6890/5975 GC/MS instrument was used (Little Falls, DE). The GC was equipped with a CIS-4 temperature programmable injector made by Gerstel Inc. (Baltimore, MD). The column used to obtain response factor data was a Restek Rxi-5MS 15 m × 0.25 mm i.d., with 0.25 μm film thickness, encased in a MACH oven (RVM Scientific, Santa Barbara, CA). The GC oven was held isothermal, 280 °C, and served to transfer sample from the injector through the MACH column to the MS. The GC column was held isothermal, 60 °C, for 1 min and ramped to 300 °C at 10 °C/min. The column head pressure was 69.84 kPa. The MACH was controlled by the Maestro software, which integrated seamlessly with Agilent's Chemstation. MACH and Maestro are sold by Gerstel. For the 1D GC/MS diesel fuel analysis, a longer, 30 m, Agilent HP-5MS column was used in a conventional oven. The oven was ramped from 60 °C (1 min) to 300 °C (5 min) at 5 °C/min under constant pressure, 30.0 kPa, programming conditions. 1 μL splitless injections were made.

The automated sequential 2D GC/MS operating condition for diesel fuel was as follows. Column 1 was an Agilent 30 m × 0.25 mm, 0.25 μm film thickness DB-1701MS, which was connected on one end to the CIS-4 inlet in the first oven and to the column flow switching device in the second oven. Column 2 was the 30 m HP-5MS column described above, housed in a separate, adjacent oven. The second column was threaded through a Gerstel CTS-2 cryotrap to focus effluent from the first column prior to thermal desorption and separation on the second column. The Maestro software controlled the sample injection, heart-cuts, freeze-trap and thermal desorption onto the second column, and the external pneumatics module for efficient sample transport to the FID and MSD could be automated. A mass flow controller in the pneumatics module provided a constant inlet flow of 10 mL/min, while a proportional valve with sensor received the outlet flow. Using Gerstel's MCS autosampler,

**Table 1**  
Patterns used to identify alkylated PAH

Isomers represented	Fragmentation pattern	Quantitative ion (%RA)	Confirmation ions (%RA)			
<b>C<sub>1</sub>-naphthalenes</b>						
1-Methyl	C <sub>1</sub> -N A <sup>a,b</sup>	142 (100)	141 (80)	115 (30)	143 (12)	
2-Methyl	C <sub>1</sub> -N B	142 (100)	141 (51)	115 (16)	143 (12)	
<b>C<sub>2</sub>-naphthalenes</b>						
1; and 2-ethyl	C <sub>2</sub> -N A <sup>a</sup>	141 (100)	156 (55)	115 (18)	142 (12)	
1,7; and 2,6-dimethyl	C <sub>2</sub> -N B <sup>a</sup>	156 (100)	141 (85)	155 (30)	115 (15)	
2,3-Dimethyl	C <sub>2</sub> -N C <sup>a,b</sup>	141 (100)	156 (98)	155 (30)	115 (23)	128 (16)
1,2; 1,3; and 1,4-dimethyl	C <sub>2</sub> -N D	156 (100)	141 (75)	155 (18)	157 (13)	115 (13)
1,5; 1,6; 1,8; and 2,7-dimethyl	C <sub>2</sub> -N E	156 (100)	141 (55)	155 (30)	115 (12)	
<b>C<sub>3</sub>-naphthalenes</b>						
1-Propyl	C <sub>3</sub> -N A <sup>a</sup>	141 (100)	170 (26)	115 (18)	142 (12)	
2-(1-Methylethyl)	C <sub>3</sub> -N B <sup>a</sup>	155 (100)	170 (30)	153 (18)	128 (17)	156 (14)
1-Methyl-8-ethyl	C <sub>3</sub> -N C <sup>a</sup>	155 (100)	170 (65)	77 (20)	153 (19)	115 (14)
Unknown isomer	C <sub>3</sub> -N D <sup>a</sup>	155 (100)	170 (55)	153 (28)	128 (20)	156 (13)
Unknown isomer	C <sub>3</sub> -N E <sup>a</sup>	170 (100)	155 (91)	153 (21)	169 (18)	171 (14)
1,4,5; and 1,4,6-trimethyl	C <sub>3</sub> -N F <sup>a,b</sup>	155 (100)	170 (75)	153 (30)	152 (25)	128 (20)
Unknown isomer	C <sub>3</sub> -N G <sup>a</sup>	141 (100)	115 (70)	170 (30)	142 (12)	
1,6,7-Trimethyl	C <sub>3</sub> -N H	170 (100)	155 (75)	169 (17)	153 (16)	171 (14)
2,3,6-Trimethyl	C <sub>3</sub> -N I	170 (100)	155 (58)	169 (17)	171 (14)	153 (11)
1-(1-Methylethyl)	C <sub>3</sub> -N J	155 (100)	128 (62)	170 (40)	115 (32)	127 (27)
<b>C<sub>4</sub>-naphthalenes</b>						
1-Methyl-7-(1-methylethyl)	C <sub>4</sub> -N A <sup>a</sup>	169 (100)	184 (50)	154 (20)	170 (15)	
1,4,5,8-Tetramethyl	C <sub>4</sub> -N B <sup>a</sup>	184 (100)	169 (68)	185 (15)	153 (12)	
1,2,3,4-Tetramethyl	C <sub>4</sub> -N C <sup>a,b</sup>	169 (100)	184 (80)	170 (14)	141 (14)	
Unknown isomer	C <sub>4</sub> -N D <sup>a</sup>	184 (100)	169 (92)	153 (21)	141 (15)	
Unknown isomer	C <sub>4</sub> -N E <sup>a</sup>	169 (100)	184 (95)	153 (25)	165 (25)	170 (15)
2-Methyl-1-propyl	C <sub>4</sub> -N F	155 (100)	184 (30)	156 (14)	153 (12)	
1-Butyl	C <sub>4</sub> -N G	141 (100)	142 (50)	184 (40)	115 (25)	
2-Butyl	C <sub>4</sub> -N H	141 (100)	142 (72)	184 (30)	115 (23)	
1-(2-Methylpropyl)	C <sub>4</sub> -N I	141 (100)	184 (30)	142 (20)	115 (10)	
2-(1,1-Dimethylethyl)	C <sub>4</sub> -N J	169 (100)	141 (46)	184 (30)	128 (17)	129 (16)
1-(1,1-Dimethylethyl)	C <sub>4</sub> -N K	169 (100)	141 (30)	184 (30)	129 (15)	128 (15)
<b>C<sub>1</sub>-fluorenes</b>						
1; and 2-methyl	C <sub>4</sub> -F A <sup>a,b</sup>	165 (100)	180 (75)	178 (25)	179 (25)	
4; and 3-methyl	C <sub>4</sub> -F B	165 (100)	180 (94)	178 (25)	179 (25)	166 (15)
9-Methyl	C <sub>4</sub> -F C	180 (100)	165 (93)	179 (22)	178 (20)	181 (15)
<b>C<sub>2</sub>-fluorenes</b>						
Unknown isomer	C <sub>2</sub> -F A <sup>a,b</sup>	194 (100)	179 (91)	89 (17)	180 (16)	
2-Ethyl and 2,3-dimethyl	C <sub>2</sub> -F B <sup>a</sup>	179 (100)	194 (80)	89 (20)	180 (17)	
Unknown isomer	C <sub>2</sub> -F C <sup>a</sup>	179 (100)	194 (65)	178 (51)	89 (25)	180 (21)
Unknown isomer	C <sub>2</sub> -F D <sup>a</sup>	165 (100)	166 (35)	194 (25)	180 (25)	
9,9; and 1,9-dimethyl	C <sub>2</sub> -F E	179 (100)	194 (40)	180 (14)	89 (10)	
9-Ethyl	C <sub>2</sub> -F F	165 (100)	194 (38)	166 (16)		
<b>C<sub>1</sub>-dibenzothiophenes</b>						
Unknown isomer	C <sub>1</sub> -D A <sup>a</sup>	198 (100)	197 (70)	199 (19)		
3-Methyl and 4-methyl	C <sub>1</sub> -D B <sup>b</sup>	198 (100)	197 (50)	199 (17)	99 (10)	
<b>C<sub>2</sub>-dibenzothiophenes</b>						
Dimethyl isomers except 1,2; 1,3; 2,3	C <sub>2</sub> -D A <sup>a,b</sup>	212 (100)	211 (45)	197 (20)	213 (17)	
1,2; 1,3; 2,3-dimethyl	C <sub>2</sub> -D B <sup>a</sup>	212 (100)	197 (55)	211 (37)	213 (25)	
Ethyl isomers	C <sub>2</sub> -D C	197 (100)	212 (52)	184 (31)		
<b>C<sub>3</sub>-dibenzothiophenes</b>						
4-Ethyl-6-methyl	C <sub>3</sub> -D A <sup>a</sup>	211 (100)	226 (78)	212 (17)	227 (13)	
1,4,8; 1,4,6; 1,2,4; 2,4,6; 2,6,7; and 3,4,6;-trimethyl	C <sub>3</sub> -D B <sup>a,b</sup>	226 (100)	211 (45)	227 (20)	212 (10)	
<b>C<sub>1</sub>-phenanthrenes</b>						
1; and 4-methyl	C <sub>1</sub> -P A <sup>a,b</sup>	192 (100)	191 (55)	189 (30)	193 (17)	190 (15)
2; 3; and 9-methyl	C <sub>1</sub> -P B	192 (100)	191 (39)	189 (20)	193 (15)	190 (10)
<b>C<sub>2</sub>-phenanthrenes</b>						
2; and 9-ethyl	C <sub>2</sub> -P A <sup>a</sup>	191 (100)	206 (70)	189 (20)	192 (20)	
9,10-Dimethyl	C <sub>2</sub> -P B <sup>a</sup>	206 (100)	191 (85)	189 (16)	89 (15)	
Unknown isomer	C <sub>2</sub> -P C <sup>a</sup>	206 (100)	191 (35)	189 (29)	205 (25)	
2,5-Dimethyl	C <sub>2</sub> -P D <sup>a,b</sup>	206 (100)	191 (51)	189 (27)	205 (20)	
3,6; 1,7; and 2,7-dimethyl	C <sub>2</sub> -P E	206 (100)	191 (20)	205 (20)	189 (17)	
2,3; and 3,5-dimethyl	C <sub>2</sub> -P F	206 (100)	191 (40)	189 (18)	205 (16)	
<b>C<sub>3</sub>-phenanthrenes</b>						
Unknown isomer	C <sub>3</sub> -P A <sup>a</sup>	205 (100)	220 (85)	189 (45)	206 (30)	204 (10)
2,3,5-Trimethyl	C <sub>3</sub> -P B <sup>a,b</sup>	220 (100)	205 (58)	189 (21)	221 (18)	101 (18)
1-Ethyl-2-methyl	C <sub>3</sub> -P C	205 (100)	220 (60)	206 (21)	189 (20)	204 (12)

<sup>a</sup> Indicates pattern found in the diesel fuel.<sup>b</sup> Indicates pattern used to calculate peak area for percent underestimated, see Table 2.

**Table 2**  
Comparison of alkylated PAH peak areas by SIM and full scan mass spectrometry using one fragmentation pattern per homolog versus spectral deconvolution of full scan data

PAH homolog	Experimental retention indices		% overestimation (SIM)	% underestimation (single pattern)
	From	To		
C <sub>1</sub> -naphthalene	216.73	227.87	0	0
C <sub>2</sub> -naphthalene	235.29	255.53	1	54
C <sub>3</sub> -naphthalene	250.47	279.15	4	12
C <sub>4</sub> -naphthalene	270.72	299.39	20	16
C <sub>1</sub> -fluorene	285.90	297.71	32	0
C <sub>2</sub> -fluorene	299.39	319.44	3	72
C <sub>1</sub> -phenanthrene	316.88	329.67	4	2
C <sub>2</sub> -phenanthrene	330.77	350.50	2	15
C <sub>3</sub> -phenanthrene	345.39	373.16	7	72
C <sub>1</sub> -dibenzothiophene	310.31	322.00	251	100
C <sub>2</sub> -dibenzothiophene	324.92	343.20	30	27
C <sub>3</sub> -dibenzothiophene	338.81	357.81	29	14

Notes: (1) The SIM signal is based on the molecular ion for each homolog. (2) The full scan signal is based on one fragmentation pattern per homolog as shown in Table 1. (3) The SIM and full scan data are compared against the peak areas obtained by the deconvolution software using the fragmentation patterns listed in Table 1 for each homolog. (4) The retention index range is used to calculate peak area differences.

1  $\mu$ L splitless injections were made. The CIS-4 was temperature programmed from 60 to 300 °C at 10 °C/s. The head pressure of the DB-1701 column was held at 122.0 kPa for 2-min and then ramped to 212 kPa at 3.7 kPa/min. The final pressure was held constant for 10 min. The first oven was held isothermal for 2 min at 60 °C and then ramped to 300 °C at 10 °C/min, with the final temperature held isothermal for 15 min. After the fourth minute, cuts were made in 1 min intervals by turning the countercurrent flow across the cross-piece off to transfer eluent to the second column, where it was frozen at –100 °C. To start the second run, the CTS-2 cold trap was heated at 25 °C/s to 300 °C. The oven temperature for the second column was identical to the 1D conditions described above.

### 2.3. Quantitation of alkylated PAH

Retention indices in this study were determined by finding alkyl PAH in all heart-cuts that matched either known patterns or those developed by the combinatorial method outlined below. These patterns, found in Table 1, were used in 1D GC/MS to determine whether or not the same peaks were found. The retention window for each homolog was chosen by subtracting or adding 0.5 min to the leading edge of the first or tail of the last peak. These times were converted to retention indices [29], setting naphthalene at 100, and phenanthrene at 200. Since chrysene was not found in the sample, we set pyrene = 352.77 based on the literature. Table 1 contains the alkylated PAH patterns used to determine the range and retention indices used in this study are in Table 2.

The Ion Signature deconvolution software is a fully functional data analysis package. It was used to extract single ion current to quantify PAH homologs. The software was also used to quantify respective homologs based on deconvolution. In the first instance the molecular ion signal was used to determine area count (area<sub>SIE</sub>). In the second, the peak area for only those peaks where the criteria for positive compound identification were met was summed (area<sub>deconvolution</sub>). The following equation was used to determine percent difference:

$$\frac{\text{area}_{\text{SIE}} - \text{area}_{\text{deconvolution}}}{\text{area}_{\text{deconvolution}}} \times 100\%$$

## 3. Results and discussion

It is customary in either SIM or full scan mass spectrometry to quantify alkylated PAH in complex samples using a single extracted ion or one fragmentation pattern per homolog. Except

for the C<sub>1</sub> homologs, reliance on a single pattern is insufficient to capture all possible isomers whether run under full scan or SIM conditions. Moreover, standard data analysis software extracts peak area without regard to common ion effects, which results in overestimating the concentration. In contrast, the deconvolution algorithms extract peak area once ion ratios for all of the scans in the peak have been evaluated and found to be within the acceptance criteria set by the user. The deconvolution procedure extracts the correct ion signal by adjusting the quant ion to the confirming ions if the matrix adds signal to the former. The converse is also true when a confirming ion is matrix affected. In this study, we identified as many alkylated PAH in diesel fuel as possible using automated sequential 2D GC/MS and the deconvolution software. Spectral patterns were grouped by homolog and used to identify isomers where no MS information was available.

### 3.1. Two-dimensional automated sequential 2D GC–GC/MS

Fig. 1 depicts the diesel fuel FID response on a DB-1701 column. Evident is the large unresolved chromatogram. Also shown are the segments, delineated by vertical lines, in which heart-cuts are made to a HP-5 column. Although unresolved total ion current (TIC) chromatograms still appear in each heart-cut, PAH are, for the most part, separated from matrix components. For example, cut 14 contains the C<sub>1</sub>- to C<sub>4</sub>-naphthalenes, which are easily separated from one another as well as the polar and aliphatic compounds in the sample except for C<sub>4</sub>-naphthalene. Although NIST or Wiley correctly identifies naphthalene (cut 12) and its C<sub>1</sub>- and C<sub>2</sub>-homologs (cut 14), not all of the C<sub>3</sub>- and C<sub>4</sub>-naphthalenes are found. Some of the missing isomers are not in the databases, while others are lost due to the matrix, which results in underestimation of these homologs.

Fig. 2 illustrates the reconstructed ion current (RIC-a) chromatogram at *m/z* 184 for the molecular ion of C<sub>4</sub>-naphthalene. The total peak area in RIC-a is much too high when compared to the peak area in RIC-b if the 1,2,3,4-tetramethylnaphthalene isomer is chosen as the surrogate for the C<sub>4</sub>-naphthalenes based solely on its ions co-maximizing. If, on the other hand, the criterion for homolog presence is based on the correct ion ratios for 1,2,3,4-tetramethylnaphthalene only the ion signal for the four peaks labeled with the pattern C are summed. In contrast, the two cuts in RIC-c make compound identification somewhat easier by removing the matrix. In this case, cut 15 shows RIC traces for three additional peaks, see pattern C. Quantitation of alkylated PAH by GC–GC is impractical, however, because ten cuts each requir-

ing a 50 min run on the second column would be necessary to identify all of the alkylated PAH homologs. This example does not account for isomers such as 2-methyl-1-propylnaphthalene and 1-butylnaphthalene whose ions differ from the surrogate and whose peak area would not be included in the total. Even the 1,4,5,8-tetramethylnaphthalene isomer would be missed since the two most abundant ions flip-flop in intensity.

### 3.2. Building libraries of alkylated PAH fragmentation patterns

We used the GC–GC/MS data to develop a library of fragmentation patterns for each homolog. According to NIST there are five unique fragmentation patterns needed to identify the 12 C<sub>2</sub>-naphthalenes if the five most abundant ions are used to make the library. From these five patterns only eight ions emerge as unique. Similarly, if the five most abundant ions for the known C<sub>4</sub>-naphthalenes are used to build libraries of fragmentation patterns for unknowns, 16 ions emerge. Because of the stability of the aromatic backbone, the molecular ion is always present and differs only in its relative abundance. Differences in functional groups and their location on PAH account for the majority of the 16 ions, which limits the number of potential high intensity ions. Selected ion extraction, adding one of the 15 ions at a time, was performed to determine which ions co-maximize with the molecular ion in heart-cuts 14 and 15. From this, many patterns emerged but it was impossible to determine whether ion profiles were invariant from one peak scan to the next using standard data analysis software. To profile the peak, at least five ions and their approximate relative abundances were entered into the deconvolution software. Because the cuts were relatively free of interferences from the matrix, the output from the software indicated which patterns produced constant relative abundances in all of the scans in a given peak.

To confirm the merit of this approach, both the GC–GC/MS and 1D mass spectral data were deconvolved and compared. The deconvolved RIC chromatogram for heart-cut 14 is shown in Fig. 3, which shows that the target ion ratios for 1-methyl-7-(1-methylethyl)naphthalene, designated as C<sub>4</sub>-N pattern A, captures the presence of three isomers and that C<sub>4</sub>-N pattern D is selective for two additional C<sub>4</sub>-naphthalenes. The figure illustrates the response when signals for the three confirming ions for each fragmentation pattern are extracted, deconvolved, and scaled to the corresponding quantitative ion (blue bar). If all of the colored bars are approximately the same height, the differences between actual and expected abundances are small. When consecutive peak scans have the same relative abundances, the scan-to-scan variability is near zero, which means each scan in the peak is similar to each other. If matrix coelution results in an enhancement of target compound signal (to the main or confirming ions), the software detects differences by measuring the scan-to-scan variability and adjusts the common ion effect based on the response of all other unaffected ions across the peak. Visualizing the data in this manner makes compound identification easy because mismatches in relative abundances are apparent. Since target ions co-maximize and have constant relative abundances for the scans in peaks at 22.92 and 23.43 min, the presence of two new C<sub>4</sub>-naphthalenes is reported. The ion ratios for C<sub>4</sub>-N pattern D fit the compound identity criteria for these two peaks while the peaks in between do not. The converse is also true, i.e., the C<sub>4</sub>-N A pattern meets the criteria for positive compound identification for the three middle peaks but results in a relative abundance mismatch for the two outside peaks in the figure. This example supports the proposition that deconvolution can be used to find new fragmentation patterns for isomers for which mass spectra do not exist. Work is in progress to isolate homolog-specific isomers from heart-cuts where MS data

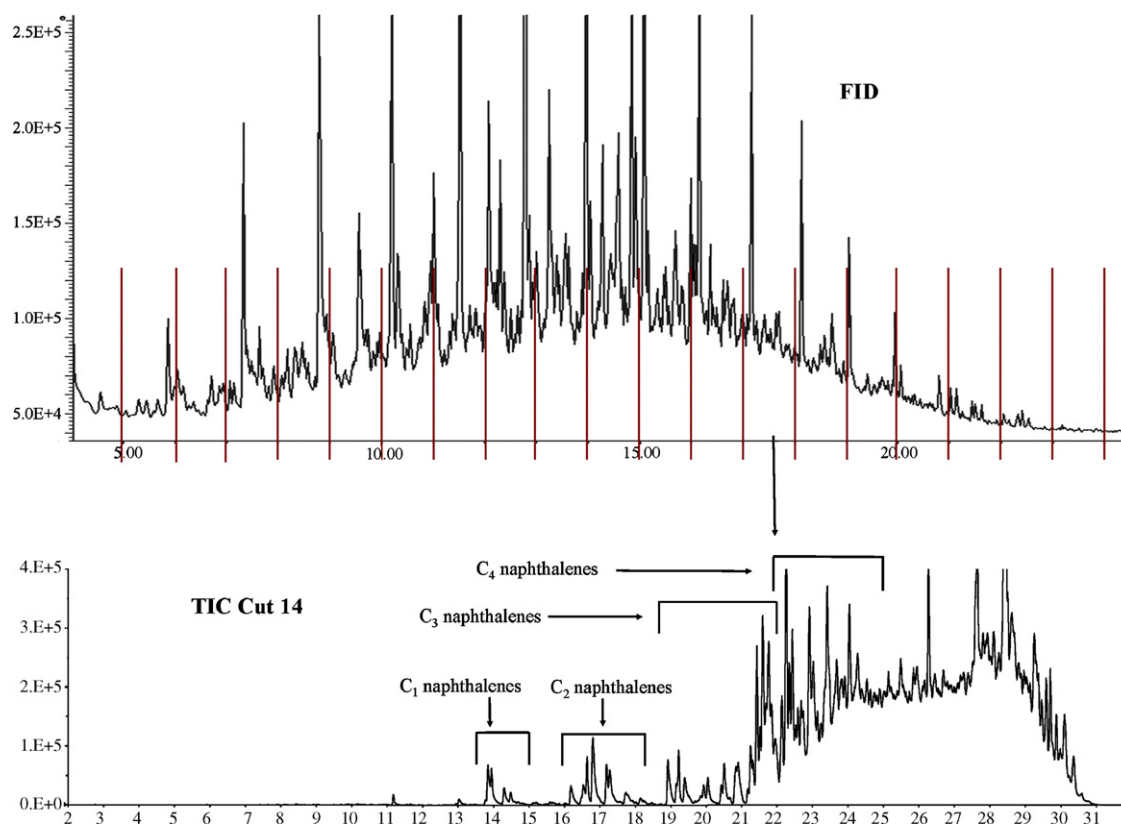


**Fig. 1.** FID trace of diesel fuel #2 on DB-1701 column, with vertical lines indicating location of heart-cuts (top). Heart-cut 14, showing C<sub>1</sub> - to C<sub>4</sub>-naphthalenes separated from the unresolved complex mixture (bottom).

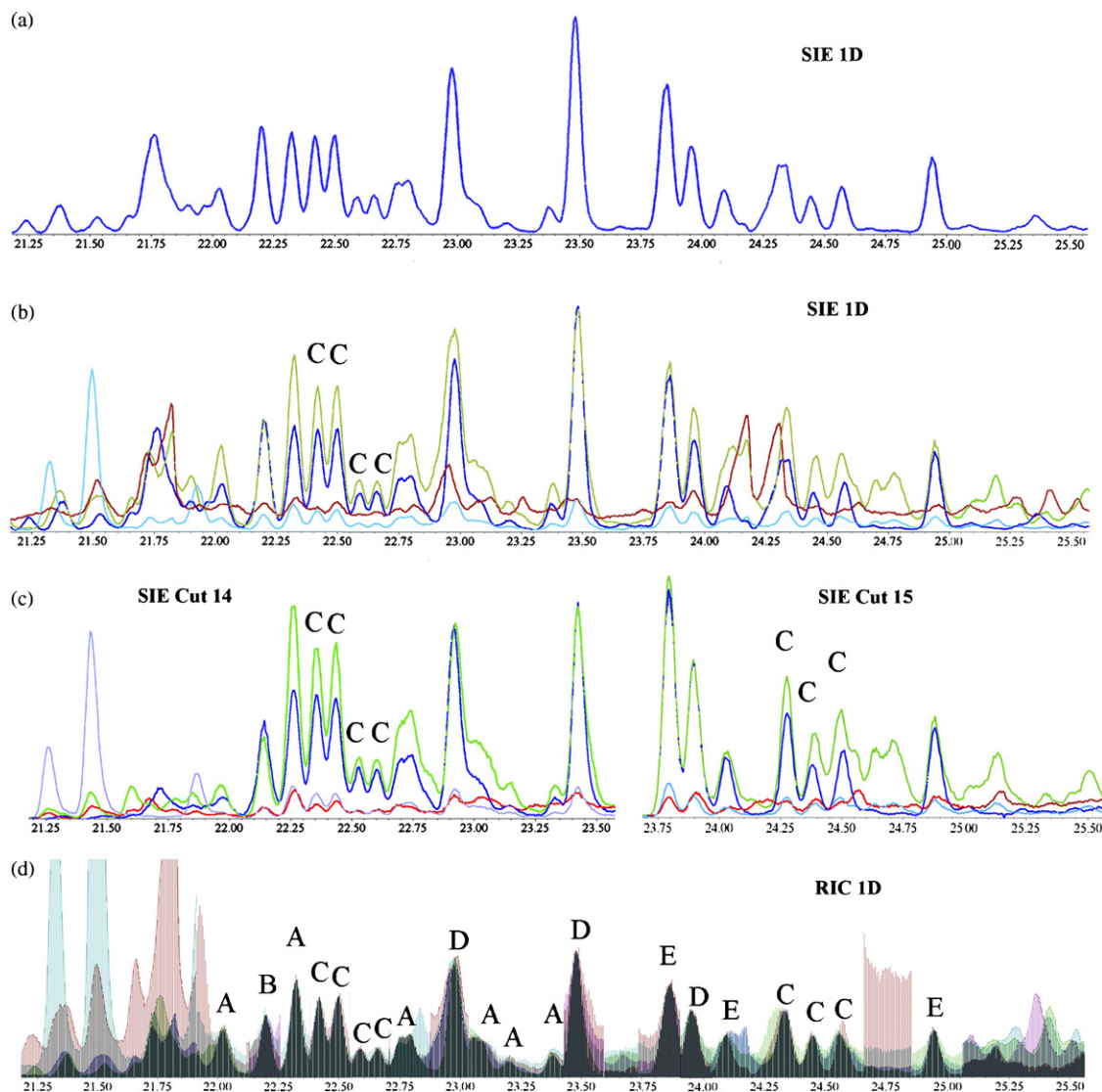


**Fig. 2.** (RIC-a) SIM chromatogram from one-dimensional GC/MS data based on  $m/z$  184, the molecular ion surrogate for  $C_4$ -naphthalenes. (RIC-b) Selected ion extraction (SIE) of 1,2,3,4-tetramethylnaphthalene as the surrogate for  $C_4$ -naphthalenes based on  $m/z$  184 (blue), 169 (light green), 170 (red), and 141 (light blue). Results obtained from one-dimensional GC/MS data. For quantitative purposes, only the peaks marked 'C' would be classified as  $C_4$ -naphthalenes since the ions at the peaks co-maximize and have the correct ion ratios. (RIC-c) Extracted ion profiles for the same ions from the GC–GC/MS data obtained from cuts 14 and 15. It is evident three additional peaks in cut 15 co-maximize and possess the correct ion ratios and should be integrated as  $C_4$ -naphthalenes. (RIC-d) Composite chromatogram obtained using the five fragmentation patterns needed to capture all of the  $C_4$ -naphthalene isomers in the diesel sample, see Table 1 for patterns.

is unavailable to confirm homolog identity by other spectroscopic techniques.

RIC-d in Fig. 2 shows the composite chromatogram for all of the  $C_4$ -naphthalenes we found in diesel fuel. A total of five patterns were needed to identify the 20 isomers found in this sample. Moreover, the Ion Signature deconvolution software identified all of the isomeric patterns in the 1D GC/MS data, including the seven  $C_4$ -naphthalene pattern C peaks, which was not possible using conventional data analysis software. The compound identification process described for  $C_4$ -naphthalene was employed for all of the alkylated PAH normally quantified in environmental forensic studies. Very little alkylated PAH for higher molecular weight homologs were found. In addition, petroleum products sourced from different crude oils may require additional patterns than those in Table 1 and, if so, the combinatorial fragmentation pattern matching approach with deconvolution and sequential 2D GC offers the best opportunity to find these compounds in extremely complex mixtures. Work

is in progress to develop a more complete list of MS fragmentation patterns using a fractionated crude oil.

### 3.3. Quantitative differences among single ion or single pattern and multiple patterns per homolog data

Table 2 lists the retention index range over which peak areas are measured and percent differences for each homolog when selected ion extraction is compared to the peak area for only those peaks found to be alkylated PAH by deconvolution. Significant overestimation occurs for  $C_4$ -naphthalene,  $C_1$ -fluorene, and the  $C_1$ - to  $C_3$ -dibenzothiophenes. Fig. 2 illustrates this finding. The peaks prior to 22 min and after 25 min are shown in RIC-a, which fall within the retention window and contribute to the  $C_4$ -naphthalene signal. In contrast, RIC-d makes clear these peaks are not alkylated PAH and should not be included in the total peak area count. Little difference in peak area count occurs among the  $C_1$  to  $C_3$ -

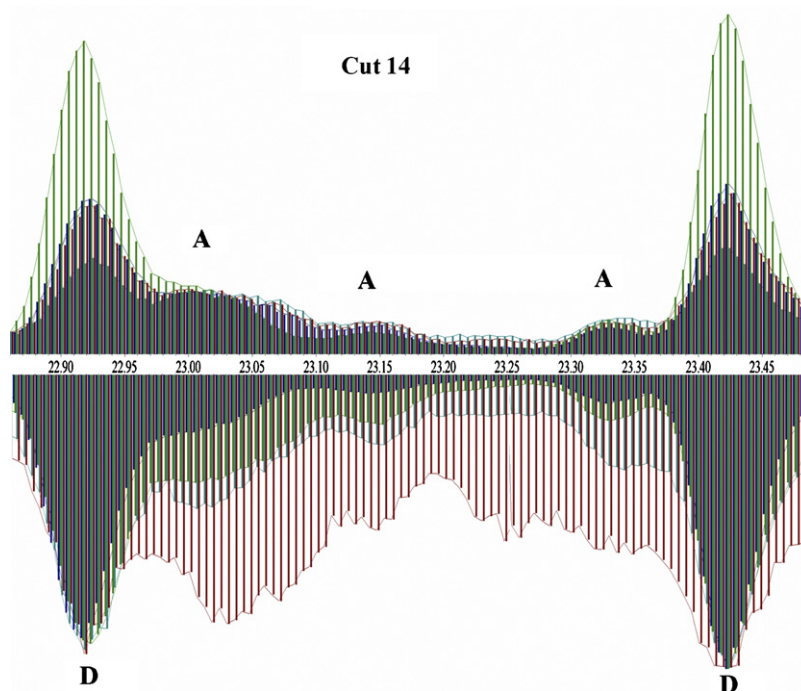


**Fig. 3.** Deconvolved ion current for  $C_4$ -naphthalene peaks as visualized in the Ion Signature Technology deconvolution software. Main and qualifier ions are each represented by colored bars at each scan, normalized to the height of the main ion. Where a set of ions are the same height, deconvolved and expected relative abundances are very close. The pattern for 1-methyl-7-(1-methylethyl)naphthalene ( $C_4$ -N A) matches the three peaks in the middle of the window shown, but not the outside two. The pattern for  $C_4$ -N D does, however, match the two outside peaks. Use of a single pattern will underestimate  $C_4$ -naphthalene abundance in the sample. Note that  $C_4$ -N D pattern is not in NIST, Wiley, or the literature and was developed by the combinatorial approach discussed in the text.

naphthalenes,  $C_2$ -fluorenes, and  $C_1$ -phenanthrenes. Too little data exists for the  $C_2$ -phenanthrenes and  $C_3$ -phenanthrenes to conclude single ion extraction produces the same data as deconvolution. Also shown in the table is the percent of the total peak area that is underestimated when one pattern per homolog is used to identify alkylated PAH compared to the patterns listed in Table 1. Evident is the loss in signal, for some >50%, when a single homolog pattern is used to quantitatively identify alkylated PAH. Higher boiling petroleum or coal tar may contain a greater diversity of compounds resulting in overestimation of signal based on single ion extraction and underestimation based on a single fragmentation pattern per alkylated family. For high throughput laboratories, spectral deconvolution of the fragmentation patterns listed in Table 1 is the only reliable method to identify all of the alkylated PAH in a complex environmental sample.

Table 3 lists the response factors for two of the three  $C_2$ -naphthalene patterns found in the diesel fuel, namely, 2,3-dimethylnaphthalene ( $C_2$ -N pattern C) and 1-ethylnaphthalene ( $C_2$ -N pattern A) as well as 1,2-dimethylnaphthalene ( $C_2$ -N pattern D), which was not found in the diesel fuel. Very different concentrations will be estimated when the same response factor is used for all isomers compared to those shown in the table. The use of a sin-

gle response factor will change dramatically the  $C_0$  to  $C_4$  homolog distribution in an environmental sample and, thus, the diagnostic ratios. If naphthalene is used as the model, our data suggests 80 compounds are needed for the  $C_0$  to  $C_4$  naphthalene, fluorene, phenanthrene, chrysene, and dibenzothiophene families. Although this is a large number of compounds, it is less than half the number in EPA method 8270 used to analyze semivolatile pollutants, but it will require the manufacture of these standards to improve the method [30,31].

#### 4. Conclusion

In this paper, we show how the Ion Signature spectral deconvolution software can be used with automated sequential 2D GC/MS in a complex mixture to provide total alkylated PAH characterization, build libraries, and identify isomers for which no MS data exists. In this regard, homologs of alkylated PAH were for the most part separated from the bulk of unresolved hydrocarbons. Based on the library of patterns, we found single ion SIM and SIE of a single homolog pattern from full scan data results in over- or underestimation of alkylated PAH concentration depending on the methodology employed compared to spectral deconvolution using multiple patterns per homolog. Our results indicate the commonly applied diagnostic ratios of  $C_2D/C_2P$  and  $C_3D/C_3P$  and their corresponding double ratio plot could lead to different conclusions, which can impact decisions being made concerning fate and transport, environmental degradation, and liability.

#### Acknowledgments

The authors greatly appreciate the assistance of Agilent Technologies, Gerstel GmbH, Gerstel USA, RVM Scientific, and Ion Signature Technology for loan or donation of equipment, supplies,

**Table 3**  
Response factors of  $C_0$  and three  $C_2$ -naphthalenes using various extracted ions for area integration

Compound	Response factor for ion		% RSD
	base ion	$m/z$ , 156	
Naphthalene	0.918	–	5.0
1-Ethylnaphthalene	1.434	0.645	6.6
1,2-Dimethylnaphthalene	1.073	0.950	7.6
2,3-Dimethylnaphthalene	1.477	1.477	7.3

and software. The support of these companies made this work possible.

## References

- [1] S.A. Stout, A.D. Uhler, K.J. McCarthy, *Environ. Forensics* 2 (2001) 87.
- [2] Z. Wang, M.F. Fingas, *Mar. Pollut. Bull.* 47 (2003) 423.
- [3] H. Alimi, T. Ertel, B. Schug, *Environ. Forensics* 4 (2003) 25.
- [4] Z. Wang, M. Fingas, *Environ. Sci. Technol.* 29 (1995) 2842.
- [5] Z. Wang, K. Li, M. Fingas, L. Sigouin, L. Menard, *J. Chromatogr. A* 971 (2002) 173.
- [6] Z. Wang, C. Yang, B. Hollebone, M. Fingas, *Environ. Sci. Technol.* 40 (2006) 5636.
- [7] R.C. Prince, D.L. Elmendorf, J.R. Lute, C.S. Hsu, C.E. Haith, J.D. Senius, G.J. Dechert, G.S. Douglas, E.L. Butler, *Environ. Sci. Technol.* 28 (1994) 142.
- [8] Z. Wang, S.A. Stout, M. Fingas, *Environ. Forensics* 7 (2006) 105.
- [9] S.A. Stout, A.D. Uhler, K.J. McCarthy, *Environ. Forensics* 6 (2005) 241.
- [10] S.A. Stout, A.D. Uhler, T.G. Naymik, K.J. McCarthy, *Environ. Sci. Technol.* 32 (1998) 260A.
- [11] F. Bertocchini, C. Vendeuvre, D. Thiebaut, *Oil Gas Sci. Technol.* 60 (2005) 937.
- [12] W. Bertsch, *J. High Resolut. Chromatogr.* 23 (2000) 167.
- [13] L. Mondello, P.Q. Tranchida, P. Dugo, G. Dugo, *Mass Spectrom. Rev.* 27 (2008) 101.
- [14] J. Dalluge, J. Beens, U.A.T. Brinkman, *J. Chromatogr. A* 1000 (2003) 69.
- [15] M. Adachour, J. Beens, R.J.J. Vreuls, U.A.T. Brinkman, *TrAC Trends Anal. Chem.* 25 (2006) 821.
- [16] O. Panic, T. Gorecki, *Anal. Bioanal. Chem.* 386 (2006) 1013.
- [17] X. Yan, *J. Chromatogr. A* 976 (2002) 3.
- [18] X. Yan, *J. Sep. Sci.* 29 (2006) 1931.
- [19] B.M. Abraham, T.Y. Liu, A. Robbat Jr., *Hazard. Waste Hazard.* 10 (1993) 461.
- [20] United States Environmental Protection Agency, Method 8270c, Section 7.5.5, 2003.
- [21] S.A. Stout, V.S. Magar, R.M. Uhler, J. Ickes, J. Abbott, R. Brenner, *Environ. Forensics* 2 (2001) 287.
- [22] Z. Wang, M. Fingas, *J. Chromatogr. A* 774 (1997) 51.
- [23] R.B. Gaines, G.J. Hall, G.S. Frysinger, W.R. Gronlund, K.L. Juare, *Environ. Forensics* 7 (2006) 77.
- [24] T. Considine, A. Robbat Jr., *Environ. Sci. Technol.* 42 (2008) 1213.
- [25] K. MacNamara, J. Howell, Y. Huang, A. Robbat Jr., *J. Chromatogr. A* 1164 (2007) 281.
- [26] Y.V. Gankin, A. Gorshteyn, S. Smarason, A. Robbat Jr., *Anal. Chem.* 70 (1998) 1655.
- [27] A. Robbat Jr., *Environ. Test. Anal.* 9 (2000) 15.
- [28] A. Robbat Jr., S. Smarason, Y.V. Gankin, *Field Anal. Chem. Tech.* 3 (1999) 55.
- [29] D.L. Vassilaros, R.C. Kong, D.W. Later, M.L. Lee, *J. Chromatogr.* 252 (1982) 1.
- [30] C.M. Reddy, J.G. Quinn, *Mar. Pollut. Bull.* 38 (1999) 126.
- [31] C.M. Reddy, J.G. Quinn, *Mar. Environ. Res.* 52 (2001) 445.